Measurement of away-side broadening with self-subtraction of flow in Au+Au collisions at $\sqrt{s_{NN}} = 200$ GeV*

J. Adam[6]   L. Adamczyk[2]   J. R. Adams[39]   J. K. Adkins[30]   G. Agakishiev[28]   M. M. Aggarwal[41]   Z. Ahammed[61]

I. Alekseev[3,35]   D. M. Anderson[55]   A. Aparin[28]   E. C. Aschenauer[6]   M. U. Ashraf[11]   F. G. Atetalla[29]   A. Attri[41]

G. S. Averichev[28]   V. Bairathi[53]   K. Barish[10]   A. Behera[52]   R. Bellwied[20]   A. Bhasin[27]   J. Bielcik[14]

J. Bielcikova[38]   L. C. Bland[6]   I. G. Bordyuzhin[3]   J. D. Brandenburg[6,49]   A. V. Brandin[35]   J. Butterworth[45]

H. Caines[64]   M. Calderón de la Barca Sánchez[8]   D. Cebra[8]   I. Chakaberia[29,6]   P. Chaloupka[14]   B. K. Chan[9]

F-H. Chang[37]   Z. Chang[6]   N. Chankova-Bunzarova[28]   A. Chatterjee[11]   D. Chen[10]   J. H. Chen[18]   X. Chen[48]

Z. Chen[49]   J. Cheng[57]   M. Cherney[13]   M. Chevalier[10]   S. Choudhury[18]   W. Christie[6]   X. Chu[6]   H. J. Crawford[7]

M. Csanád[16]   M. Daugherity[1]   T. G. Dedovich[28]   I. M. Deppner[19]   A. A. Derevschikov[43]   L. Didenko[6]   X. Dong[31]

J. L. Drachenberg[1]   J. C. Dunlop[6]   T. Edmonds[44]   N. Elsey[63]   J. Engelage[7]   G. Eppley[45]   S. Esumi[58]

O. Evdokimov[12]   A. Ewigleben[32]   O. Eyser[6]   R. Fatemi[30]   S. Fazio[6]   P. Federic[38]   J. Fedorisin[28]   C. J. Feng[37]

Y. Feng[44]   P. Filip[28]   E. Finch[51]   Y. Fisyak[6]   A. Francisco[64]   L. Fulek[2]   C. A. Gagliardi[55]   T. Galatyuk[15]

F. Geurts[45]   A. Gibson[60]   K. Gopal[23]   D. Grosnick[60]   W. Guryn[6]   A. I. Hamad[29]   A. Hamed[5]   S. Harabasz[15]

J. W. Harris[64]   S. He[11]   W. He[18]   X. H. He[26]   S. Heppelmann[8]   S. Heppelmann[42]   N. Herrmann[19]   E. Hoffman[20]

L. Holub[14]   Y. Hong[31]   S. Horvat[64]   Y. Hu[18]   H. Z. Huang[9]   S. L. Huang[52]   T. Huang[37]   X. Huang[57]

T. J. Humanic[39]   P. Huo[52]   G. Igo[9]   D. Isenhower[1]   W. W. Jacobs[25]   C. Jena[23]   A. Jentsch[6]   Y. Ji[48]   J. Jia[6,52]

K. Jiang[48]   S. Jowzaee[63]   X. Ju[48]   E. G. Judd[7]   S. Kabana[53]   M. L. Kabir[10]   S. Kagamaster[32]   D. Kalinkin[25]

K. Kang[57]   D. Kapukchyan[10]   K. Kauder[6]   H. W. Ke[6]   D. Keane[29]   A. Kechechyan[28]   M. Kelsey[31]

Y. V. Khyzhniak[35]   D. P. Kikoła[62]   C. Kim[10]   B. Kimelman[8]   D. Kincses[16]   T. A. Kinghorn[8]   I. Kisel[17]

A. Kiselev[6]   M. Kocan[14]   L. Kochenda[35]   L. K. Kosarzewski[14]   L. Kramarik[14]   P. Kravtsov[35]   K. Krueger[4]

N. Kulathunga Mudiyanselage[20]   L. Kumar[41]   S. Kumar[26]   R. Kunnawalkam Elayavalli[63]   J. H. Kwasizur[25]

R. Lacey[52]   S. Lan[11]   J. M. Landgraf[6]   J. Lauret[6]   A. Lebedev[6]   R. Lednicky[28]   J. H. Lee[6]   Y. H. Leung[31]

C. Li[48]   W. Li[50]   W. Li[45]   X. Li[48]   Y. Li[57]   Y. Liang[29]   R. Licenik[38]   T. Lin[55]   Y. Lin[11]   M. A. Lisa[39]   F. Liu[11]

H. Liu[25]   P. Liu[52]   P. Liu[50]   T. Liu[64]   X. Liu[39]   Y. Liu[55]   Z. Liu[48]   T. Ljubicic[6]   W. J. Llope[63]

R. S. Longacre[6]   N. S. Lukow[54]   S. Luo[12]   X. Luo[11]   G. L. Ma[50]   L. Ma[18]   R. Ma[6]   Y. G. Ma[50]   N. Magdy[12]

R. Majka[64]   D. Mallick[36]   S. Margetis[29]   C. Markert[56]   H. S. Matis[31]   J. A. Mazer[46]   N. G. Minaev[43]

S. Mioduszewski[55]   B. Mohanty[36]   I. Mooney[63]   Z. Moravcova[14]   D. A. Morozov[43]   M. Nagy[16]   J. D. Nam[54]

Nasim Md.[22]   K. Nayak[11]   D. Neff[9]   J. M. Nelson[7]   D. B. Nemes[64]   M. Nie[49]   G. Nigmatkulov[35]   T. Niida[58]

L. V. Nogach[43]   T. Nonaka[58]   A. S. Nunes[6]   G. Odyniec[31]   A. Ogawa[6]   S. Oh[31]   V. A. Okorokov[35]   B. S. Page[6]

R. Pak[6]   A. Pandav[36]   Y. Panebratsev[28]   B. Pawlik[40]   D. Pawlowska[62]   H. Pei[11]   C. Perkins[7]   L. Pinsky[20]

R. L. Pintér[16]   J. Pluta[62]   J. Porter[31]   M. Posik[54]   N. K. Pruthi[41]   M. Przybycien[2]   J. Putschke[63]   H. Qiu[26]

A. Quintero[54]   S. K. Radhakrishnan[29]   S. Ramachandran[30]   R. L. Ray[56]   R. Reed[32]   H. G. Ritter[31]

O. V. Rogachevskiy[28]   J. L. Romero[8]   L. Ruan[6]   J. Rusnak[38]   N. R. Sahoo[49]   H. Sako[58]   S. Salur[46]   J. Sandweiss[64]

S. Sato[58]   W. B. Schmidke[6]   N. Schmitz[33]   B. R. Schweid[52]   F. Seck[15]   J. Seger[13]   M. Sergeeva[9]   R. Seto[10]

P. Seyboth[33]   N. Shah[24]   E. Shahaliev[28]   P. V. Shanmuganathan[6]   M. Shao[48]   A. I. Sheikh[29]   F. Shen[49]

W. Q. Shen[50]   S. S. Shi[11]   Q. Y. Shou[50]   E. P. Sichtermann[31]   R. Sikora[2]   M. Simko[38]   J. Singh[41]   S. Singha[26]

N. Smirnov[64]   W. Solyst[25]   P. Sorensen[6]   H. M. Spinka[4]   B. Srivastava[44]   T. D. S. Stanislaus[60]   M. Stefaniak[62]

D. J. Stewart[64]   M. Strikhanov[35]   B. Stringfellow[44]   A. A. P. Suaide[47]   M. Sumbera[38]   B. Summa[42]   X. M. Sun[11]

X. Sun[12]   Y. Sun[48]   Y. Sun[21]   B. Surrow[54]   D. N. Svirida[3]   P. Szymanski[62]   A. H. Tang[6]   Z. Tang[48]

A. Taranenko[35]   T. Tarnowsky[34]   J. H. Thomas[31]   A. R. Timmins[20]   D. Tlusty[13]   M. Tokarev[28]   C. A. Tomkiel[32]

S. Trentalange[9]   R. E. Tribble[55]   P. Tribedy[6]   S. K. Tripathy[16]   O. D. Tsai[9]   Z. Tu[6]   T. Ullrich[6]

D. G. Underwood[4]   I. Upsal[49,6]   G. Van Buren[6]   J. Vanek[38]   A. N. Vasiliev[43]   I. Vassiliev[17]   F. Videbæk[6]

S. Vokal[28]   S. A. Voloshin[63]   F. Wang[44]   G. Wang[9]   J. S. Wang[21]   P. Wang[48]   Y. Wang[11]   Y. Wang[57]

Z. Wang[49]   J. C. Webb[6]   P. C. Weidenkaff[19]   L. Wen[9]   G. D. Westfall[34]   H. Wieman[31]   S. W. Wissink[25]

R. Witt[59]   Y. Wu[10]   Z. G. Xiao[57]   G. Xie[31]   W. Xie[44]   H. Xu[21]   N. Xu[31]   Q. H. Xu[49]   Y. F. Xu[50]   Y. Xu[49]

Z. Xu[6]   Z. Xu[9]   C. Yang[49]   Q. Yang[49]   S. Yang[6]   Y. Yang[37]   Z. Yang[11]   Z. Ye[45]   Z. Ye[12]   L. Yi[49]   K. Yip[6]

H. Zbroszczyk[62]   W. Zha[48]   C. Zhang[52]   D. Zhang[11]   S. Zhang[48]   S. Zhang[50]   X. P. Zhang[57]   Y. Zhang[48]

Y. Zhang[11]   Z. J. Zhang[37]   Z. Zhang[6]   Z. Zhang[12]   J. Zhao[44]   C. Zhong[50]   C. Zhou[50]   X. Zhu[57]   Z. Zhu[49]

M. Zurek[31]   M. Zyzak[17]   (STAR Collaboration)

[1]Abilene Christian University, Abilene, Texas 79699
[2]AGH University of Science and Technology, FPACS, Cracow 30-059, Poland
[3]Alikhanov Institute for Theoretical and Experimental Physics NRC "Kurchatov Institute", Moscow 117218, Russia
[4]Argonne National Laboratory, Argonne, Illinois 60439
[5]American University of Cairo, New Cairo 11835, New Cairo, Egypt
[6]Brookhaven National Laboratory, Upton, New York 11973
[7]University of California, Berkeley, California 94720
[8]University of California, Davis, California 95616
[9]University of California, Los Angeles, California 90095
[10]University of California, Riverside, California 92521
[11]Central China Normal University, Wuhan, Hubei 430079
[12]University of Illinois at Chicago, Chicago, Illinois 60607
[13]Creighton University, Omaha, Nebraska 68178
[14]Czech Technical University in Prague, FNSPE, Prague 115 19, Czech Republic
[15]Technische Universität Darmstadt, Darmstadt 64289, Germany
[16]ELTE Eötvös Loránd University, Budapest, Hungary H-1117
[17]Frankfurt Institute for Advanced Studies FIAS, Frankfurt 60438, Germany
[18]Fudan University, Shanghai 200433
[19]University of Heidelberg, Heidelberg 69120, Germany
[20]University of Houston, Houston, Texas 77204
[21]Huzhou University, Huzhou, Zhejiang 313000
[22]Indian Institute of Science Education and Research (IISER), Berhampur 760010 , India
[23]Indian Institute of Science Education and Research (IISER) Tirupati, Tirupati 517507, India
[24]Indian Institute Technology, Patna, Bihar 801106, India
[25]Indiana University, Bloomington, Indiana 47408
[26]Institute of Modern Physics, Chinese Academy of Sciences, Lanzhou, Gansu 730000
[27]University of Jammu, Jammu 180001, India
[28]Joint Institute for Nuclear Research, Dubna 141 980, Russia
[29]Kent State University, Kent, Ohio 44242
[30]University of Kentucky, Lexington, Kentucky 40506-0055
[31]Lawrence Berkeley National Laboratory, Berkeley, California 94720
[32]Lehigh University, Bethlehem, Pennsylvania 18015
[33]Max-Planck-Institut für Physik, Munich 80805, Germany
[34]Michigan State University, East Lansing, Michigan 48824
[35]National Research Nuclear University MEPhI, Moscow 115409, Russia
[36]National Institute of Science Education and Research, HBNI, Jatni 752050, India
[37]National Cheng Kung University, Tainan 70101
[38]Nuclear Physics Institute of the CAS, Rez 250 68, Czech Republic
[39]Ohio State University, Columbus, Ohio 43210
[40]Institute of Nuclear Physics PAN, Cracow 31-342, Poland
[41]Panjab University, Chandigarh 160014, India
[42]Pennsylvania State University, University Park, Pennsylvania 16802
[43]NRC "Kurchatov Institute", Institute of High Energy Physics, Protvino 142281, Russia
[44]Purdue University, West Lafayette, Indiana 47907
[45]Rice University, Houston, Texas 77251
[46]Rutgers University, Piscataway, New Jersey 08854
[47]Universidade de São Paulo, São Paulo, Brazil 05314-970

[48]University of Science and Technology of China, Hefei, Anhui 230026
[49]Shandong University, Qingdao, Shandong 266237
[50]Shanghai Institute of Applied Physics, Chinese Academy of Sciences, Shanghai 201800
[51]Southern Connecticut State University, New Haven, Connecticut 06515
[52]State University of New York, Stony Brook, New York 11794
[53]Instituto de Alta Investigación, Universidad de Tarapacá, Chile
[54]Temple University, Philadelphia, Pennsylvania 19122
[55]Texas A&M University, College Station, Texas 77843
[56]University of Texas, Austin, Texas 78712
[57]Tsinghua University, Beijing 100084
[58]University of Tsukuba, Tsukuba, Ibaraki 305-8571, Japan
[59]United States Naval Academy, Annapolis, Maryland 21402
[60]Valparaiso University, Valparaiso, Indiana 46383
[61]Variable Energy Cyclotron Centre, Kolkata 700064, India
[62]Warsaw University of Technology, Warsaw 00-661, Poland
[63]Wayne State University, Detroit, Michigan 48201
[64]Yale University, New Haven, Connecticut 06520

Abstract: High transverse momentum (p_T) particle production is suppressed owing to the parton (jet) energy loss in the hot dense medium created in relativistic heavy-ion collisions. Redistribution of energy at low-to-modest p_T has been difficult to measure, owing to large anisotropic backgrounds. We report a data-driven method for background evaluation and subtraction, exploiting the away-side pseudorapidity gaps, to measure the jetlike correlation shape in Au+Au collisions at $\sqrt{s_{NN}}$ = 200 GeV in the STAR experiment. The correlation shapes, for trigger particles $p_T > 3$ GeV/c and various associated particle p_T ranges within $0.5 < p_T < 10$ GeV/c, are consistent with Gaussians, and their widths increase with centrality. The results indicate jet broadening in the medium created in central heavy-ion collisions.

Keywords: di-hadron correlations, jet, heavy-ion

DOI: 10.1088/1674-1137/ab97a9

1   Introduction

The basic constituents of nuclear matter are quarks and gluons. Their interactions are governed by the rules of quantum chromodynamics (QCD). QCD matter, normally confined into hadrons, is deconfined into a state of matter known as the quark-gluon plasma (QGP) under extreme conditions of high energy/matter densities [1]. A QGP phase existed in the early universe and is also created in heavy-ion collisions at the relativistic heavy-ion collider (RHIC) [2-5] and the large hadron collider (LHC) [6]. One important piece of evidence for the discovery of the QGP is jet quenching, i.e. parton (jet) energy loss in the QGP medium, which in relativistic heavy-ion collisions suppresses high transverse momentum (p_T) particle and jet production [7-16]. The suppression is so strong that a density at least 30-fold the normal nuclear density is required for describing data in model calculations [17].

The partonic energy loss mechanisms are, however, less clear. Some models focus on collisional and radiative energy losses [17]. Others propose more exotic mechanisms, such as collective excitation modes [18-23]. While single-particle measurements are not sufficiently sensitive to energy loss mechanisms, measurements of

the lost energy's redistribution at low to modest p_T are expected to be more sensitive. One approach is to reconstruct jets and study p_T and angular distributions of jet fragments [24-26]. Distributions of the lost energy can also be measured via dihadron angular correlations with respect to high-p_T trigger particles and jets. Previous measurements of two- and multi-particle correlations, after subtracting elliptic flow background, have revealed novel correlation structures [27-31]. However, owing to initial collision geometry fluctuations, all orders of harmonics (not just elliptic) flow anisotropies are possible [32, 33]. Full subtraction of anisotropic backgrounds is challenging and suffers from large uncertainties [24, 31, 34-43].

Here, we devise a data-driven method with an "automatic" subtraction of anisotropic flow backgrounds. The method was first tested with toy model and PYTHIA simulations [44]. Although the correlated jetlike yield cannot be readily determined using this method, the correlation shape can be obtained without the large uncertainty associated with the flow subtraction. We study the correlation shape as a function of the collision centrality and associated particle p_T. The correlation shape should be sensitive to the nature of jet-medium interactions, and therefore offers new opportunities to investigate energy

loss mechanisms and medium properties.

2   Experiment and data

The data reported here were collected in 2011 in the STAR experiment using a minimum bias (MB) trigger in Au+Au collisions at the nucleon-nucleon center-of-mass energy of $\sqrt{s_{NN}} = 200$ GeV. The MB trigger is defined by a coincidence signal between the east and west vertex position detectors (VPDs) [45] located at the pseudorapidity range of $4.4 < |\eta| < 4.9$. Overall, 3.2×10^8 MB trigger events are used. The event centrality is defined by the measured charged particle multiplicity within $|\eta| < 0.5$. Data are reported in four centrality bins, corresponding to 0-10%, 10%-30%, 30%-50%, and 50%-80% of the total hadronic cross-section [46].

The main detector used for this analysis is the time projection chamber (TPC) [47, 48], residing in a 0.5 T magnetic field along the beam direction (z). Particle tracks are reconstructed in the TPC and are required to have at least 20 out of 45 maximally possible hits. The ratio of the number of hits used in the track reconstruction to the number of possible hits is required to be above 0.51, for eliminating multiple track segments being reconstructed from a single particle trajectory. The primary vertex (PV) is reconstructed using tracks. Events with the PV position (z_{vtx}) within 30 cm of the TPC center along z are used. To remove secondaries from particle decays, only tracks with the distance of closest approach DCA <2 cm to the PV are used.

3   Analysis method

Jetlike correlations are studied with respect to high-p_T trigger particles, which serve as proxies for jets [17, 31]. High-p_T particles measured at RHIC are strongly biased toward the surface of the collision zone [17, 49, 50]. The away-side jet partner, which is preferentially directed inward, is therefore very likely to traverse the entire volume, suffering maximal interactions with the medium. Because of the broad distribution of the underlying parton kinematics, the away-side jet direction is mostly uncorrelated in η relative to the trigger particle [31]. It is therefore difficult to distinguish the jet signal from the underlying background; the large, azimuthally anisotropic background has to be *specifically* subtracted, with large uncertainties, traditionally using measured anisotropy parameters [31]. The away-side jet direction can be localized by requiring a second high-p_T particle back-to-back in the azimuthal angle (ϕ) with respect to the first one. However, by doing so, the back-to-back dijets are biased towards being tangential to the collision zone [41, 51], substantially weakening the purpose of studying jet-medi-

um interactions.

In this analysis, we impose a less biasing requirement of a large recoil transverse momentum (P_x) azimuthally opposite to the high-p_T trigger particle, within a given η range, to enhance the away-side jet population in the acceptance. The schematic diagram in Fig. 1 shows the away-side $\eta - \phi$ space and illustrates by the fading gray area the away-side jet population enhanced in a particular η regoin. P_x is given by

$$P_x|_{\eta_1}^{\eta_2} = \sum_{\eta_1 < \eta < \eta_2, |\phi - \phi_{\text{trig}}| > \pi/2} p_T \cos(\phi - \phi_{\text{trig}}) \cdot \frac{1}{\epsilon}, \qquad (1)$$

where all charged particles ($0.15 < p_T < 10$ GeV/c) within the η range that are on the away side ($|\phi - \phi_{\text{trig}}| > \pi/2$) of the trigger particle are included. Since the near-side jet is not included in the P_x calculation, the η distribution of the trigger particle is unbiased by the P_x cut. The inverse of the single-particle relative acceptance×efficiency (ϵ) is used to correct for the single-particle detection efficiency. It depends on the position of the primary vertex along the beam axis z_{vtx}, collision centrality, particle p_T, η and ϕ, and has run period variations [46]. The ϕ-dependence of ϵ_ϕ is obtained, separately for positive and negative η, from the single-particle ϕ distribution normalized to unity on average in each centrality. The η-dependence of ϵ varies with z_{vtx}, centrality and p_T, and is obtained by treating symmetrized dN/dη distribution in events with $|z_{vtx}| < 2$ cm as the baseline, and taking the ratio of the dN/dη distribution from each z_{vtx} bin to this baseline. Because our P_x cut is only used to select a given fraction of events, the absolute efficiency correction is not applied.

In this analysis the trigger particle p_T range is $3 < p_T^{\text{trig}} < 10$ GeV/c. We choose the windows $-1 < \eta < -0.5$ or $0.5 < \eta < 1$ for P_x calculation. Figure 2 shows example $P_x|_{0.5}^1$ distributions for peripheral and central Au+Au collisions. Their difference comes mainly from
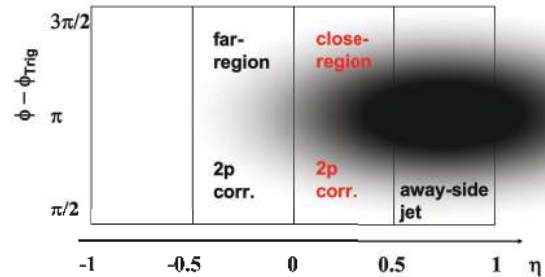

Fig. 1.   (color online) Schematic of the analysis method. The requirement of a large recoil P_x [Eq. (1)] in a particular η region $(0.5 < \eta < 1$ shown here) selects events with enhanced population of jets close to the η region. Jetlike correlations in the close-region and far-region, symmetric with respect to midrapidity, contain different contributions from the jet but the same contribution from the flow background. Their difference measures the jetlike correlation shape.
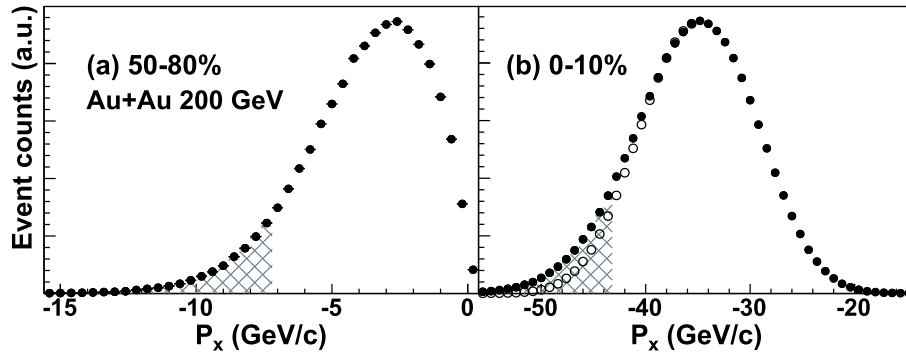
Fig. 2.   Distributions of the recoil momentum within $0.5 < \eta < 1$ ($P_x|_{0.5}^1$) from high-p_T trigger particles of $3 < p_T^{\text{trig}} < 10$ GeV/c in (a) 50%-80% peripheral and (b) 0-10% central collisions. The shaded areas indicate a selection of 10% of events to enhance the away-side jet population inside acceptance. Events from $|z_{\text{vtx}}| < 2$ cm are used; other z_{vtx} events and $P_x|_{-1}^{-0.5}$ are similar. The right side of the P_x distribution is reflected to the left of the maximum, with open circles.

event multiplicities. For each centrality, we select the 10% of the events with the highest $-P_x$ to enhance the probability that the away-side jet population is contained in this η region. There is a large statistical fluctuation effect in P_x, especially in central collisions. The P_x selection may also be affected by low-p_T minijets. These effects do not strictly give a symmetric distribution [44]. Nevertheless, we show the reflected data as open circles in Fig. 2(b) to give an order of magnitude estimate of those effects.

In the selected events, we analyze dihadron correlations of associated particles, with respect to trigger particles, in two η regions symmetric with respect to midrapidity, one close ("close-region") to and the other far ("far-region") from the η window for P_x(Fig. 1). The dihadron correlation in $\Delta\phi = \phi_{\text{assoc}} - \phi_{\text{trig}}$, between the associated and trigger particle azimuthal angles, is given by

$$\frac{\mathrm{d}N}{\mathrm{d}\Delta\phi} = \frac{1}{N_{\text{trig}}} \cdot \frac{S(\Delta\phi)}{B(\Delta\phi)/B_0} , \qquad (2)$$

where

$$S(\Delta\phi) = \int_{-1}^{+1} \mathrm{d}\eta_{\text{trig}} \int_{\text{region}} \mathrm{d}\eta_{\text{assoc}} \frac{\mathrm{d}^3 N}{\mathrm{d}\eta_{\text{trig}}\mathrm{d}\eta_{\text{assoc}}\mathrm{d}\Delta\phi} \cdot \frac{1}{\epsilon} \qquad (3)$$

and $B(\Delta\phi)$ is its counterpart from mixed events. The correlations are normalized by the number of trigger particles, N_{trig}. In Eq. (3), "region" stands for close-region or far-region. All the trigger particles with $|\eta_{\text{trig}}| < 1$ are integrated. The single-particle relative acceptance×efficiency (ϵ) correction is applied to associated particles. As in the case of P_x, the absolute efficiency correction is not applied in the correlation measurements because this analysis deals with only the correlation shape, not the absolute amplitude. The mixed-events are formed by pairing the trigger particles in each event with the associated particles from 10 different random events in the same centrality and z_{vtx} bin. The mixed-event background

$B(\Delta\phi)$ is normalized to unity (via the constant B_0), to correct for residual two-particle acceptance after single-particle efficiency correction.

The away-side jet contributes more to the close region than to the far region, owing to the larger $\Delta\eta$ gap of the latter (Fig. 1). The anisotropic flow contributions, on the other hand, are on average equal in these two regions that are symmetric with respect to midrapidity. The difference in the close- and far-region correlations, therefore, arises only from jetlike correlations. For $P_x|_{-1}^{-0.5}$, the close-region is $-0.5 < \eta < 0$ and the far-region is $0 < \eta < 0.5$; for $P_x|_{0.5}^1$, they are swapped. The results from these two sets are consistent, and thus combined. We exclude events where both $P_x|_{-1}^{-0.5}$ and $P_x|_{0.5}^1$ satisfy the respective 10% P_x cut, because the combined signal would be strictly zero but with a propagated nonzero statistical error.

PYTHIA simulations [44] indicate that jet fragmentations are approximately factorized in η and ϕ. The $\Delta\phi$ correlations at different $\Delta\eta$ have approximately the same shape, only differing in magnitude. Thus, the difference between close- and far-region correlations measures the away-side correlation shape. We quantify the shape by a Gaussian width σ determined by fitting.

4   Systematic uncertainties

The systematic uncertainties of σ come from several sources. Varying the P_x cut changes the relative contributions of jets and background fluctuations to selected events, but should not affect the correlation width significantly if the jet sample is unbiased. We vary the P_x cut from allowing the default 10% of events to 2%, 5%, 15%, 20%, 30% and 50% of events. The calculated systematic uncertainty of σ is 3.4% (one standard deviation).

We have assumed that jetlike correlations are factorized in η and ϕ. There is theoretical [52-54] and experi-

mental evidence [55] that flow may be decorrelated over η , owing to geometry fluctuations. Both these effects would cause uncertainties in attributing the close- and far-region difference purely to jetlike correlations. We vary the close- and far-region η locations and ranges so they have different η gaps in between as well as from the P_x η window, but are still symmetric with respect to midrapidity. We also vary the P_x η window location and range. The largest deviation of σ from the default results is approximately half of the statistical error. The calculated systematic uncertainty of σ is 2.0% (one standard deviation) for this source.

In addition, we vary the track quality cuts in the analysis. The calculated systematic uncertainty for this source is 5.3% standard deviation in σ. The final systematic uncertainty is calculated as the quadratic sum of all the sources we studied.

The systematic uncertainties on σ are found to be partially correlated between various centralities and p_T^{assoc} bins. In the difference between central and peripheral collisions, $\Delta\sigma = \sqrt{\sigma_{\mathrm{cent}}^2 - \sigma_{\mathrm{peri}}^2}$, the systematic uncertainties are not simply propagated but obtained in the same way as those on the individual σ's described above. The same procedure is used to obtain the systematic uncertainty on the linear parameterization of $\Delta\sigma$ versus p_T^{assoc}.

5   Results and discussion

Figure 3(a) shows, as an example, the dihadron azimuthal correlations for the close-region and far-region in 10%-30% Au+Au collisions at $\sqrt{s_{NN}} = 200$ GeV for trigger $3 < p_T^{\mathrm{trig}} < 10\,\mathrm{GeV/c}$ and associated particle $1 < p_T^{\mathrm{assoc}} < 2\,\mathrm{GeV/c}$. The near-side correlations are almost identical for close- and far-region. The near-side ratio of far- to close-region correlations, α, are listed in Table 1 and are all approximately unity. This indicates, to a good degree, that near-side jetlike correlations are not biased by the P_x selection and flow contributions to close- and far-region correlations are indeed equal.

The away-side correlations differ in amplitude and shape, which is caused by the away-side jet contributions. The far-region correlation is scaled by α to account for the small near-side difference and then we subtract it from the close-region correlation. The result is shown in Fig. 3(b). The difference measures the away-side jetlike correlation shape. A Gaussian fit centered at $\Delta\phi = \pi$ is used, for extracting the correlation width. The χ^2 values per degree of freedom are all consistent with unity, indicating that the correlation shape is Gaussian. The σ values are tabulated in Table 2.

Figure 4 shows the away-side correlation width (Gaussian σ) as a function of centrality, for five p_T^{assoc} bins. The width for the lowest p_T^{assoc} of 0.15-0.5 GeV/c is
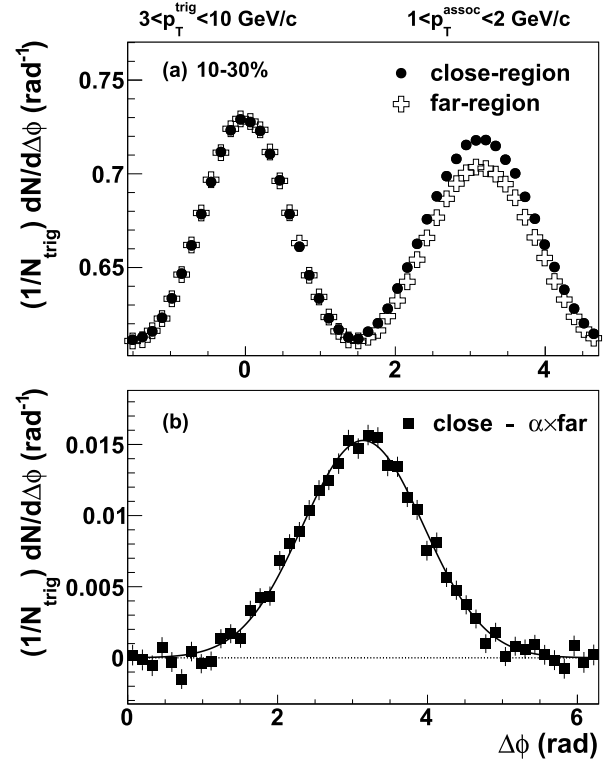

Fig. 3.   (a) Dihadron azimuthal correlations in close-region (solid circles) and far-region (open crosses), as an example, for $3 < p_T^{\mathrm{trig}} < 10\,\mathrm{GeV/c}$ and $1 < p_T^{\mathrm{assoc}} < 2\,\mathrm{GeV/c}$ in 10%-30% Au+Au collisions at $\sqrt{s_{NN}} = 200$ GeV. (b) The difference between close-region correlation and scaled far-region correlation (see text for detail). The curve is a Gaussian fit with the centroid fixed at π. Errors are statistical.

consistent with a constant over centrality; at this low p_T^{assoc}, the correlations are fairly wide for all centralities, and possible broadening with increasing centrality may not be easily observable. For the four higher p_T^{assoc} bins, the width increases from peripheral to central collisions. The broadening of the correlation function is consistent with jet broadening. However, it is also possible, because the correlation measurement is statistical, that the broadening comes from an increasing dijet acoplanarity (nuclear k_T effect [56, 57]) with increasing centrality. One possible mechanism of the nuclear k_T effect is multiple scattering by incident nucleons before the hard scattering between underlying partons. The nuclear k_T effect gives the hard scattering partons an initial net momentum in the transverse plane, and thus causes a spread in the dijet angular correlation.
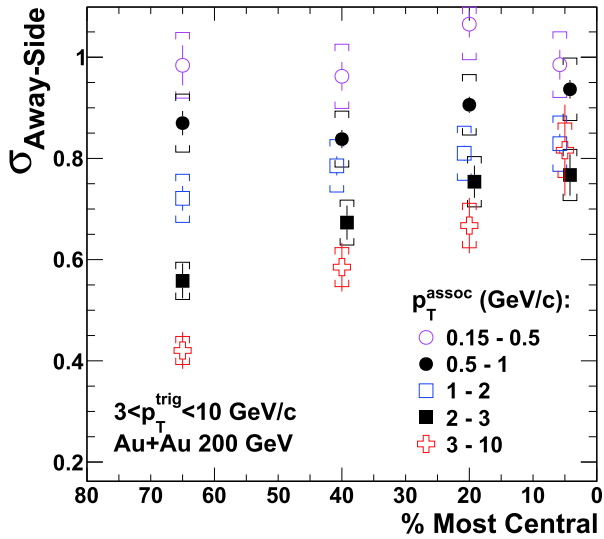
Figure 5(a) shows σ as a function of p_T^{assoc} in peripheral and central collisions. In peripheral collisions, the width decreases rapidly with increasing p_T^{assoc}. In central collisions the decrease is less rapid. We quantify the broadening from peripheral to central collisions by $\Delta\sigma = \sqrt{\sigma_{\mathrm{cent}}^2 - \sigma_{\mathrm{peri}}^2}$, shown as a function of p_T^{assoc} in Fig.

Table 1.   The near-side ratio of far- to close-region correlations, α, averaged over $|\Delta\phi| < 1$ as a function of p_T^{assoc} and centrality in Au+Au collisions at $\sqrt{s_{NN}} = 200$ GeV. The trigger particle has $3 < p_T^{trig} < 10$ GeV/c. Errors are statistical.
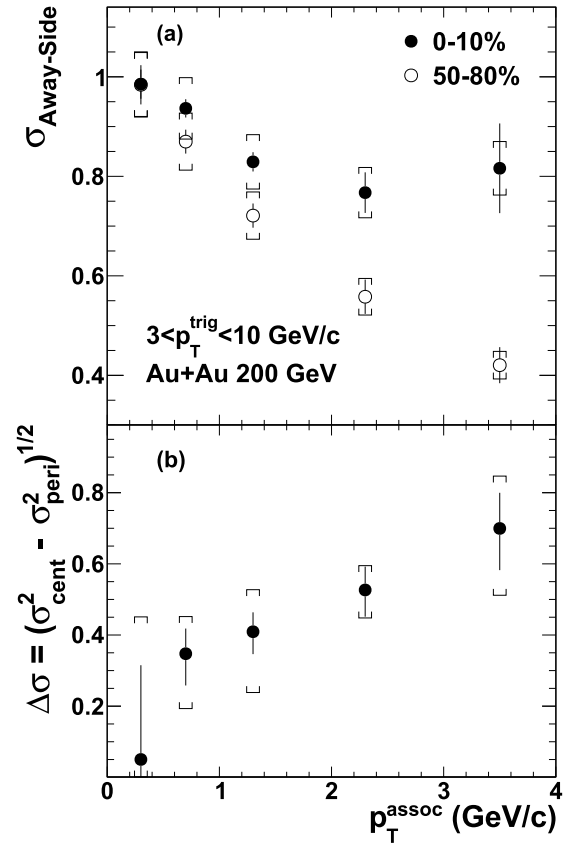
p_T^{assoc} /(GeV/c)	50%-80%	30%-50%	10%-30%	0-10%
0.15-0.5	1.0038 ± 0.0007	1.0036 ± 0.0003	1.0027 ± 0.0001	1.0002 ± 0.0001
0.5-1	1.000 ± 0.001	1.0021 ± 0.0003	1.0006 ± 0.0002	0.9984 ± 0.0001
1-2	1.002 ± 0.002	1.0002 ± 0.0006	0.9994 ± 0.0003	0.9976 ± 0.0002
2-3	0.997 ± 0.006	1.006 ± 0.002	0.9995 ± 0.0009	0.9965 ± 0.0008
3-10	0.99 ± 0.01	0.999 ± 0.005	0.998 ± 0.003	0.999 ± 0.003

Table 2.   Gaussian fit width to away-side jetlike correlations as a function of p_T^{assoc} and centrality in Au+Au collisions at $\sqrt{s_{NN}} = 200$ GeV. The trigger particle has $3 < p_T^{trig} < 10$ GeV/c. The first error is statistical and the second is systematic.

p_T^{assoc} /(GeV/c)	50%-80%	30%-50%	10%-30%	0-10%
0.15-0.5	$0.98 \pm 0.04 \pm 0.06$	$0.96 \pm 0.03 \pm 0.06$	$1.07 \pm 0.03 \pm 0.07$	$0.99 \pm 0.03 \pm 0.06$
0.5-1	$0.87 \pm 0.02 \pm 0.06$	$0.84 \pm 0.02 \pm 0.06$	$0.91 \pm 0.02 \pm 0.06$	$0.94 \pm 0.03 \pm 0.06$
1-2	$0.72 \pm 0.02 \pm 0.05$	$0.79 \pm 0.02 \pm 0.05$	$0.81 \pm 0.02 \pm 0.05$	$0.83 \pm 0.02 \pm 0.06$
2-3	$0.56 \pm 0.03 \pm 0.04$	$0.67 \pm 0.03 \pm 0.04$	$0.75 \pm 0.03 \pm 0.05$	$0.77 \pm 0.04 \pm 0.05$
3-10	$0.42 \pm 0.04 \pm 0.03$	$0.59 \pm 0.05 \pm 0.04$	$0.67 \pm 0.05 \pm 0.04$	$0.82 \pm 0.09 \pm 0.05$

Fig. 4.   (color online) Away-side jetlike correlation width (Gaussian σ) as a function of centrality (0 indicates the most central collisions) for $3 < p_T^{trig} < 10$ GeV/c and various p_T^{assoc} bins in Au+Au collisions at $\sqrt{s_{NN}} = 200$ GeV. Bars are statistical errors and caps are systematic uncertainties.

Fig. 5.   (a) Away-side jetlike correlation width as a function of p_T^{assoc} for $3 < p_T^{trig} < 10$ GeV/c in 50%-80% peripheral (open circles) and top 10% central (solid circles) Au+Au collisions at $\sqrt{s_{NN}} = 200$ GeV. (b) The difference between the correlation widths in central and peripheral collisions. Bars are statistical errors and caps are systematic uncertainties.

5(b). The relative broadening is stronger for higher p_T associated particles. At very low p_T^{assoc}, the jetlike correlation is already quite broad in peripheral collisions, limiting any further broadening in central collisions. At high p_T^{assoc} the initial jetlike correlation is narrow, leaving significant room for broadening in central collisions. In previous STAR dihadron correlation measurements [5, 30], the reported away-side correlations were broader than those reported here, likely because the previous results did not have the high-order harmonic flow backgrounds

subtracted. We also note that the reported jet-hadron correlations [40] were measured with a much higher jet p_T and the extracted widths at low p_T^{assoc} suffer from large flow background uncertainties.

If the away-side correlation broadening is owing to the nuclear k_T effect only, without medium-induced jet broadening, then we would have $\sigma_{\mathrm{cent}}^2 = \sigma_{\mathrm{peri}}^2 + \sigma_{k_T}^2$. Here, k_T quantifies the dijet acoplanarity and should ideally not depend on the associated particle p_T^{assoc}. With the wide p_T^{trig} range, it is possible that a higher p_T^{assoc} could bias towards higher p_T^{trig}, hence smaller k_T effect. To investigate this quantitatively, we fit the data in Fig. 5(b) by a linear function, yielding $\Delta\sigma = (0.23\pm0.09(\mathrm{stat.})\pm0.11(\mathrm{syst.}))+ (0.13\pm0.04(\mathrm{stat.})\pm0.05(\mathrm{syst.}))p_T$ (p_T in GeV/c). This suggests that the nuclear k_T effect (expected constant or decreasing with p_T^{assoc}) is not the only source for the observed broadening. There must be contributions from a p_T dependent effect such as medium induced jet broadening. This conclusion is corroborated by the relatively small nuclear k_T measured by both PHENIX [58, 59] and STAR [60, 61] We note that the measured broadening is between the associated and trigger particle angles, not directly the angle of the jet fragment from the jet axis. It is the combination of broadening at the trigger particle p_T and the associated particle p_T values.

A more explicit means to distinguish the jet-medium broadening from the k_T effect and other possible mechanisms is to use three-particle correlations [62, 63]. With our method of subtracting anisotropic flow backgrounds, three-particle correlations could shed new light on partonic energy loss mechanisms in relativistic heavy-ion collisions. We leave such studies to future investigations.

6   Conclusions

We have reported a measurement of away-side jet-like azimuthal correlation shapes relative to a high-p_T trigger particle ($3 < p_T^{\mathrm{trig}} < 10$ GeV/c) in Au+Au collisions at $\sqrt{s_{NN}} = 200$ GeV by the STAR experiment. We devised a method for a clean and robust subtraction of anisotropic flow backgrounds, using the correlation data itself. Namely, we enhance the away-side jet population in the acceptance by requiring a large recoil momentum P_x (Eq. (1)), and take the difference of jetlike correlations in regions symmetric with respect to midrapidity but with different $\Delta\eta$ gaps away from the enhanced P_x region. The measured Gaussian width of the away-side jetlike correlation increases with increasing centrality in the associated particle p_T range of $0.5 < p_T^{\mathrm{assoc}} < 10$ GeV/c. The increase is consistent with the medium-induced jet broadening of the trigger and/or associated particles in addition to the nuclear k_T effect.

References

1   E. V. Shuryak, Phys. Lett. B, **78**: 150 (1978)
2   I. Arsene *et al*. (BRAHMS Collaboration), Nucl. Phys. A, **757**: 1 (2005), arXiv:nucl-ex/0410020
3   B. Back *et al*. (PHOBOS Collaboration), Nucl. Phys. A, **757**: 28 (2005), arXiv:nucl-ex/0410022
4   K. Adcox *et al*. (PHENIX Collaboration), Nucl. Phys. A, **757**: 184 (2005), arXiv:nucl-ex/0410003
5   J. Adams *et al*. (STAR Collaboration), Nucl. Phys. A, **757**: 102 (2005), arXiv:nucl-ex/0501009
6   B. Muller, J. Schukraft, and B. Wyslouch, Ann. Rev. Nucl. Part. Sci., **62**: 361 (2012), arXiv:1202.3233
7   K. Adcox *et al*. (PHENIX Collaboration), Phys. Rev. Lett., **88**: 022301 (2002), arXiv:nucl-ex/0109003
8   C. Adler *et al*. (STAR Collaboration), Phys. Rev. Lett., **89**: 202301 (2002), arXiv:nucl-ex/0206011
9   C. Adler *et al*. (STAR Collaboration), Phys. Rev. Lett., **90**: 082302 (2003), arXiv:nucl-ex/0210033
10   J. Adams *et al*. (STAR Collaboration), Phys. Rev. Lett., **91**: 172302 (2003), arXiv:nucl-ex/0305015
11   S. Adler *et al*. (PHENIX Collaboration), Phys. Rev. Lett., **91**: 072303 (2003), arXiv:nucl-ex/0306021
12   S. Adler *et al*. (PHENIX Collaboration), Phys. Rev. Lett., **91**: 072301 (2003), arXiv:nucl-ex/0304022
13   J. Adams *et al*. (STAR Collaboration), Phys. Rev. Lett., **91**: 072304 (2003), arXiv:nucl-ex/0306024
14   G. Aad *et al*. (ATLAS Collaboration), Phys .Rev. Lett., **105**: 252303 (2010), arXiv:1011.6182
15   S. Chatrchyan *et al*. (CMS Collaboration), Phys. Rev. C, **84**: 024906 (2011), arXiv:1102.1957
16   K. Aamodt *et al*. (ALICE Collaboration), Phys.Lett. B, **696**: 30 (2011), arXiv:1012.1004
17   P. Jacobs and X.-N. Wang, Prog. Part. Nucl. Phys., **54**: 443 (2005), arXiv:hep-ph/0405125
18   H. Stoecker, Nucl. Phys. A, **750**: 121 (2005), arXiv:nuclth/0406018
19   J. Casalderrey-Solana, E. Shuryak, and D. Teaney, J. Phys. Conf. Ser., **27**: 22 (2005), arXiv:hep-ph/0411315
20   G.-L. Ma and X.-N. Wang, Phys. Rev. Lett., **106**: 162301 (2011), arXiv:1011.5249
21   Y. Tachibana and T. Hirano, Phys. Rev. C, **90**: 021902 (2014), arXiv:1402.6469
22   Y. Tachibana and T. Hirano, Phys. Rev. C, **93**: 054907 (2016), arXiv:1510.06966
23   Y. Tachibana, N.-B. Chang, and G.-Y. Qin, Phys. Rev. C, **95**: 044909 (2017), arXiv:1701.07951
24   A. Adare *et al*. (PHENIX Collaboration), Phys. Rev. Lett., **111**: 032301 (2013), arXiv:1212.3323
25   V. Khachatryan *et al*. (CMS Collaboration), JHEP, **02**: 156 (2016), arXiv:1601.00079
26   S. Chatrchyan *et al*. (CMS Collaboration), Phys. Lett. B, **730**: 243 (2014), arXiv:1310.0878
27   J. Adams *et al*. (STAR Collaboration), Phys. Rev. Lett., **95**: 152301 (2005), arXiv:nucl-ex/0501016
28   S. Adler *et al*. (PHENIX Collaboration), Phys. Rev. Lett., **97**: 052301 (2006), arXiv:nucl-ex/0507004
29   A. Adare *et al*. (PHENIX Collaboration), Phys. Rev. C, **78**:

014901 (2008), arXiv:0801.4545

30 M. Aggarwal *et al*. (STAR Collaboration), Phys. Rev. C, **82**: 024912 (2010), arXiv:1004.2377

31 F. Wang, Prog. Part. Nucl. Phys., **74**: 35 (2014), arXiv:1311.4444

32 B. Alver and G. Roland, Phys. Rev.C, **81**: 054905(2010), erratum-ibid. C82, 039903(2010), 1003.0194.

33 U. Heinz and R. Snellings, Ann. Rev. Nucl. Part. Sci., **63**: 123 (2013), arXiv:1301.2826

34 H. Agakishiev *et al*. (STAR Collaboration) (2010), 1010.0690.

35 H. Agakishiev *et al*. (STAR), Phys. Rev. C, **89**: 041901 (2014), arXiv:1404.1070

36 A. Adare *et al*. (PHENIX), Phys. Rev. C, **99**: 054903 (2019), arXiv:1803.01749

37 K. Aamodt *et al*. (ALICE Collaboration), Phys. Rev. Lett., **108**: 092301 (2012), arXiv:1110.0121

38 J. Adam *et al*. (ALICE Collaboration), Phys. Lett. B, **763**: 238 (2016), arXiv:1608.07201

39 L. Adamczyk *et al*. (STAR Collaboration), Phys. Lett. B, **760**: 689 (2016), arXiv:1604.01117

40 L. Adamczyk *et al*. (STAR Collaboration), Phys. Rev. Lett., **112**: 122301 (2014), arXiv:1302.6184

41 L. Adamczyk *et al*. (STAR), Phys. Rev. C, **87**: 044903 (2013), arXiv:1212.1653

42 G. Agakishiev *et al*. (STAR Collaboration), Phys. Rev. C, **85**: 014903 (2012), arXiv:1110.5800

43 B. Abelev *et al*. (STAR Collaboration), Phys. Rev. C, **94**: 014910 (2016), arXiv:1603.05477

44 L. Zhang, K. Jiang, C. Li *et al*., Phys. Rev. C, **100**: 014903 (2019), arXiv:1902.06027

45 W. Llope, F. Geurts, J. Mitchell *et al*., Nucl. Instrum. Meth. A, **522**: 252 (2004), arXiv:nucl-ex/0308022

46 B. Abelev *et al*. (STAR Collaboration), Phys. Rev. C, **79**: 034909

(2009), arXiv:0808.2041

47 K. Ackermann *et al*. (STAR Collaboration), Nucl. Phys. A, **661**: 681 (1999)

48 M. Anderson *et al*., Nucl. Instrum. Meth. A, **499**: 659 (2003), arXiv:nucl-ex/0301015

49 H. Zhang, J. F. Owens, E. Wang *et al*., Phys. Rev. Lett., **98**: 212301 (2007), arXiv:nucl-th/0701045

50 T. Renk, Phys. Rev. C, **88**: 054902 (2013), arXiv:1212.0646

51 H. Agakishiev *et al*. (STAR), Phys. Rev. C, **83**: 061901 (2011), arXiv:1102.2669

52 P. Bozek, W. Broniowski, and J. Moreira, Phys. Rev. C, **83**: 034911 (2011), arXiv:1011.3354

53 K. Xiao, F. Liu, and F. Wang, Phys. Rev. C, **87**: 011901 (2013), arXiv:1208.1195

54 J. Jia and P. Huo, Phys. Rev. C, **90**: 034915 (2014), arXiv:1403.6077

55 V. Khachatryan *et al*. (CMS), Phys. Rev. C, **92**: 034911 (2015), arXiv:1503.01692

56 J. W. Cronin, H. J. Frisch, M. J. Shochet *et al*., Phys. Rev. D, **11**: 3105 (1975)

57 I. Vitev, J. Phys. G, **31**: S557 (2005), arXiv:hep-ph/0409297

58 J. Rak, J. Phys. G, **30**: S1309 (2004), arXiv:hep-ex/0403038

59 S. Adler *et al*. (PHENIX Collaboration), Phys.Rev. D, **74**: 072002 (2006), arXiv:hep-ex/0605039

60 T. Henry (STAR), Acta Phys. Hung. A, **27**: 217 (2006), arXiv:nucl-ex/0511002

61 J. Putschke (STAR), Nucl. Phys. A, **830**: 58C (2009), arXiv:0908.1766

62 B. Abelev *et al*. (STAR Collaboration), Phys. Rev. Lett., **102**: 052302 (2009), arXiv:0805.0622

63 B. Abelev *et al*. (STAR Collaboration), Phys. Rev. Lett., **105**: 022301 (2010), arXiv:0912.3977